

# METALLURGICAL EVALUATION OF DISSIMILAR METAL JOINTS FOR ACCELERATOR VACUUM CHAMBER CONSTRUCTION AT THE ADVANCED PHOTON SOURCE UPGRADE PROJECT \*

G. Navrotski<sup>†</sup> and B. Brajuskovic, Advanced Photon Source,  
Argonne National Laboratory, Argonne, Illinois, 60439 USA

## Abstract

Tubular vacuum chamber assemblies made of aluminum, copper and stainless steel alloys will be used in the new Multi Bend Achromat (MBA) storage ring that is being developed at Advanced Photon Source (APS). Details of the new lattice magnet system design and ring impedance considerations continue to drive these vacuum chambers to smaller dimensions and thinner walls with tighter geometric tolerances under higher thermal loads. It is important to carefully evaluate the methods used to join these dissimilar metal components looking for compromise in primary strength, permeability, electrical and thermal properties while still creating structures that are ultra-high vacuum compatible and leak-tight. This paper visually details the underlying metallurgical changes that occur when joining various combinations of aluminum, OFE copper, GlidCop<sup>®</sup> and stainless steel using brazing, bonding and welding techniques. Each of the techniques has its advantages and disadvantages with engineering and economic consequences.

## VACUUM BRAZING

To support the accelerator systems development program, a series of vacuum test coupons of a style shown in Fig. 1 were prepared and evaluated. The exact sample shown below includes a 316L stainless steel (UNS S31603) CF flange to GlidCop-Al15<sup>®</sup> (UNS C15715) vacuum braze (left end), a GlidCop<sup>®</sup> to OFE copper (UNS C10100) TIG weld (left center) and a stainless to OFE copper braze (right).

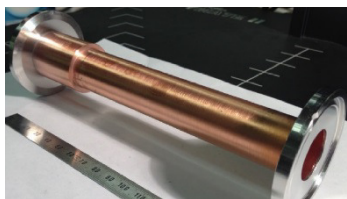


Figure 1: Typical dissimilar metal test coupon.

Joining two different materials using a third intermediate substance that bonds well to both is a highly developed and mature technology. For ultra-high vacuum (UHV) component fabrication using dissimilar metals, vacuum brazing is

the ‘gold standard’ by which other techniques are measured.

A magnified cross-section of a OFE copper to 316L stainless steel vacuum joint is shown in Fig. 2. Both metals are well wet and fused by the gold braze alloy. Excess braze both inside and outside of the joint has a clean well-

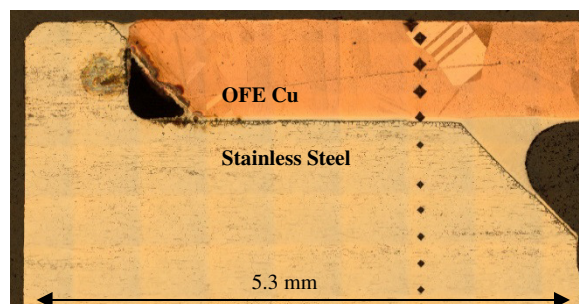


Figure 2: Vacuum braze of stainless to OFE copper.

formed meniscus without voids. The joint design, specifically the chamfer on the OFE copper, creates an unintended trapped volume and potential virtual leak in the component. There has been tremendous grain growth in the copper during processing. Microhardness tests (small diamond indents) show that, as expected, the copper has become fully annealed from its original work-hardened condition.

A similar braze of GlidCop-Al15<sup>®</sup> to 316L stainless steel is shown in Fig. 3. The reader should carefully consult the literature for the exacting conditions required for GlidCop<sup>®</sup> brazing [1, 2]. Both metals are nicely wetted and well bonded. There are a few insignificant voids present in the braze metal layer. Microhardness tests confirm that both the stainless and GlidCop<sup>®</sup> retain their full base metal strength properties, unaltered by the brazing process.



Figure 3: Stainless steel to GlidCop<sup>®</sup> vacuum braze.

\* Funding provided by the Advanced Photon Source, U.S. Department of Energy, Office of Science, Argonne National Laboratory under Contract No. DE-AC02-06CH11357

<sup>†</sup> email address: Navrotski@anl.gov

## E-BEAM WELDING

Electron beam welding in vacuum is an alternative dissimilar metal joining technique. Figure 4 shows a cross-section of a full penetration e-beam weld joining OFE copper to 316L stainless steel. The two metals are linked by a complex intermetallic mixture and are well fused. Microhardness and grain size measurements confirm that the heat affected zone does not extend through the full 4 mm of copper. The vacuum (top) surface of the copper tube maintains 85% of its as-received, work hardened strength transitioning to a fully annealed condition at the mid-line position.

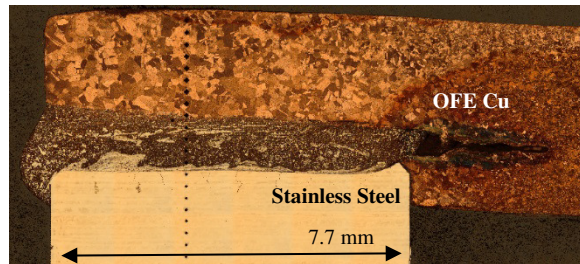


Figure 4: E-beam weld of stainless to OFE copper.

There are two negative consequences to imparting the high energy densities needed for this 8 mm deep weld. First, the process creates a three-millimetre-deep weld-root void in the copper. This should not be a factor for vacuum integrity nor for impedance but, as an internal stress concentration source, the void could be a factor in structural considerations. Secondly, the stainless steel has a very high level of induced and retained residual stress. Symptoms of this residual stress state can be seen in the series of small, almost equidistant 500  $\mu\text{m}$  deep stress cracks in the stainless steel flange metal.

Very similar observations are made on the full penetration e-beam weld of GlidCop<sup>®</sup> to 316L stainless steel shown in Fig. 5. That is to say; the metals are well fused by a complex intermixture, there is a large weld-root void and there are high levels of residual stress in the stainless steel.

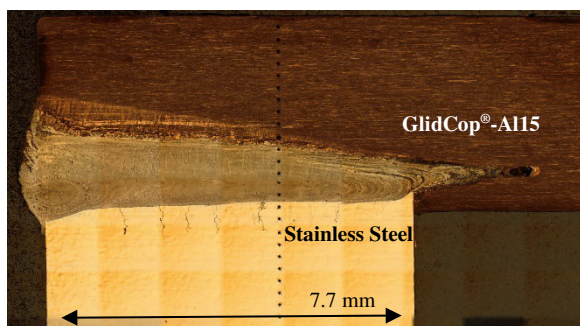


Figure 5: E-beam weld of stainless to GlidCop<sup>®</sup>.

Unlike the previous case with OFE copper, the GlidCop<sup>®</sup> strength is unaffected by the welding process except for a narrow band of recrystallized material (light copper band), especially near the weld face and weld toe. In this region the GlidCop<sup>®</sup> has lost half of its strength.

Figure 6 shows a typical microstructure for an electron beam weld joining OFE copper (left) to GlidCop<sup>®</sup> (right). Microstructural regions in this sample are more complex. Reviewing the image from left to right, note the cold-worked base metal OFE grain structure (A), a recrystallized copper zone (B), a region copper grain growth (C), the e-beam weld bead (D) with conspicuous grain flow pattern, a thin region of GlidCop<sup>®</sup> recrystallization (E) and GlidCop<sup>®</sup>-Al15 base metal (F). The reader is advised to ignore the surface cracks on the under-bead side (top surface this view) of the weld as a preparation artifact. Microhardness measurements across the weld confirm a highly asymmetric heat affected zone. The region between

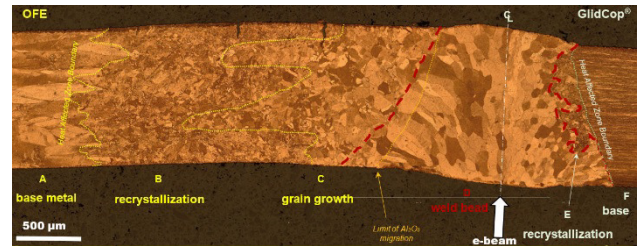


Figure 6: E-beam weld of OFE to GlidCop<sup>®</sup>.

the two base metals (A) and (F) has been highly annealed. To the left of the approximately 1 mm wide weld bead centerline, the OFE copper has been annealed to a distance of 4 mm. To the right of the centerline, the GlidCop<sup>®</sup> has only annealed within a thin < 500  $\mu\text{m}$  recrystallized region.

A word of caution is necessary. On numerous other occasions, e-beam welds of GlidCop<sup>®</sup> have shown a chronic tendency to form both gas voids at the weld-bead center and interface voids at the weld-bead to recrystallized GlidCop<sup>®</sup> interface as shown in Fig. 7. If this were another type of welding, gas entrainment from the atmosphere ( $\text{N}_2$  or  $\text{O}_2$ ) or gas generation by wet surfaces ( $\text{H}_2$ ) would normally be blamed. In the vacuum electron-beam process there are no such sources. It is conjectured, without proof, that the e-beam welding process itself could be disassociating the  $\text{Al}_2\text{O}_3$  dispersoids present in the GlidCop<sup>®</sup> creating Al, which readily dissolves into the copper matrix, and  $\text{O}_2$ , which coalesces into the observed gas pockets.

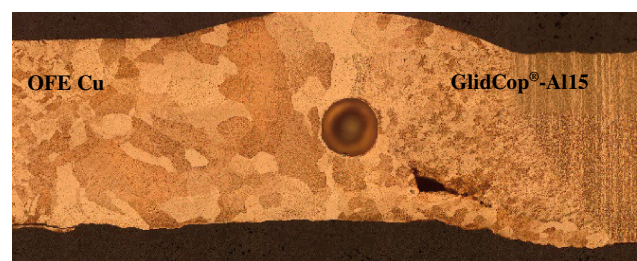


Figure 7: Problems in OFE to GlidCop<sup>®</sup> e-beam welds.

Overall, electron beam welding shows great promise for dissimilar metal joining needed in accelerator vacuum chamber construction. As with all welding methods, careful quality control over surface preparation, beam power, penetration depth and post-weld inspection are needed for each different configuration.



## TIG WELDING

Tungsten inert gas (TIG) welding of OFE copper to GlidCop® and its extremely wide heat affected zone is shown in contrast to the e-beam case above. Figure 8 shows the central 5 mm of a typical TIG weld. To the left of the TIG centreline is the OFE side of the weld bead with large fully annealed grain structure. To the right is the weld bead and 1.33 mm of recrystallized GlidCop®. A single large and numerous small interface voids are seen at the weld bead to recrystallized GlidCop® interface.

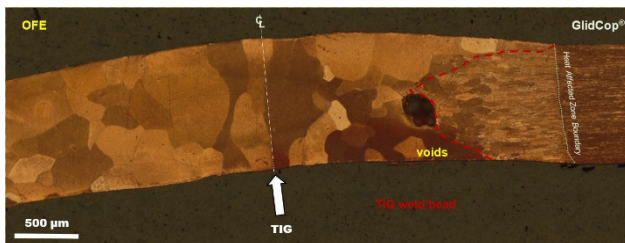


Figure 8: TIG weld of OFE to GlidCop®.

The heat affected zone on the OFE side of the weld extends to 33 mm from the weld bead centerline. The corresponding heat affected zone on the GlidCop® side is limited to the 1.3 mm region recrystallized material delimited by the white dashed line. The welds are vacuum tight but design must account for low mechanical strength over many cm of annealed material and potential midline voids.

## LASER WELDING

Industrial lasers provide another source of welding power. With focusing, they have an advantage of being used either in vacuum or in a controlled atmosphere. Figure 9 shows a 50% penetration, capping weld of a 316L stainless steel to a thin wall OFE copper tubing. The input power is sufficient to fully anneal the copper for the full 8 mm length of the weld preparation. Copper recrystallization and large grain growth near the weld bead can be seen.

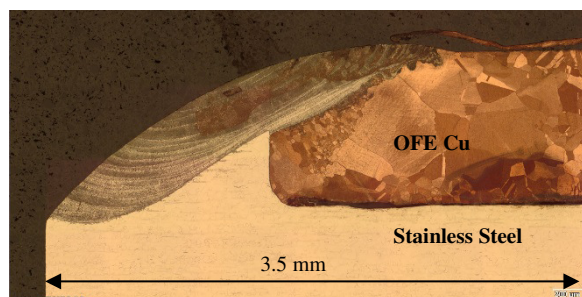


Figure 9: Laser weld of stainless to OFE copper.

Scalloped layering from consecutive laser pulses can be seen in the weld bead. Pockets of intermixed copper are also visible. The two metals are well fused and vacuum tight but the specific design of this joint provides only ~450 µm of brittle intermetallic weld material between the UHV conditions inside the accelerator chamber (top in this photo) and the continuous crevice leak to atmosphere along

the OFE / stainless interface. With an improved weld design and further power controls, laser welding is a viable option, both technically and economically, for fusing dissimilar metal components for synchrotron applications.

## FRICTION WELDING

Spin friction welding of an aluminum alloy tube to a 316L stainless steel tube is shown in Fig. 10. The interface is sharp and vacuum tight. On the aluminum (left) side, a 600 µm band the metallurgical structure has been highly modified to a fine grain condition with a 20% decrease of strength. The stainless steel (right) remains unaltered. Although the interface is extremely sharp and continuous with no noticeable melting, the reader will note a uniform 4 µm wide region between the two 'forged' surfaces. This band contains altered material that was preferentially removed during the metallographic electropolishing. Further investigation is warranted but the technique shows great promise for accelerator vacuum chamber fabrication.

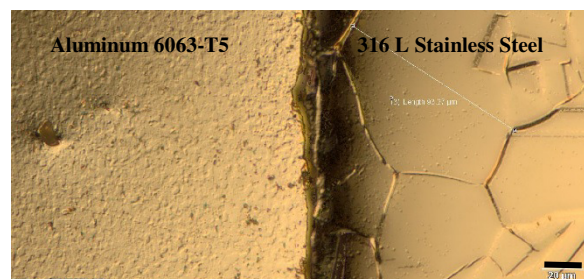


Figure 10: Friction weld of aluminum to stainless.

## EXPLOSION BONDING

Explosion bonding is also a reliable but somewhat expensive option for dissimilar metal joining. A compatible dissimilar metal couple is created as seen in Fig. 11 by the explosion bonding process and fabricated into a coupling component. Only traditional similar-to-similar metal welding is then required fabricate the assembly. Careful materials design considered is required to choose an appropriate stack of explosion-bonded coupling materials.

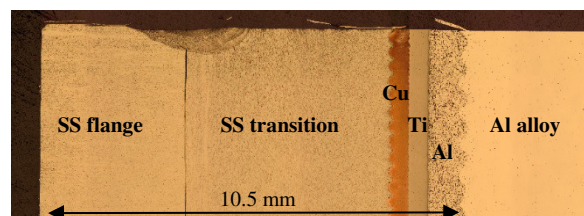


Figure 11: Explosion bonding interface.

## REFERENCES

- [1] P.K. Samal, "Brazing and Diffusion Bonding of Glidcop® Dispersion Strengthened Copper," The Metal Science of Joining, edited by M.J. Cieslak et al., Minerals, Metals & Materials Society, 1992.
- [2] W. Toter and S. Sharma, "Analysis of Gold-Copper Braze Joints in Glidcop® for UHV Components at the Advanced Photon Source" MEDSI (2004)